EUROPEAN ORGANIZATION FOR NUCLEAR RESEARCH

CERN - SL DIVISION

CERN-SL-95-110

CERN-SL-95-110 AP

SL 9550

IMPROVING THE DYNAMIC APERTURE OF LEP2

Y. Alexahin*

Abstract

A variety of means to improve the dynamic aperture of LEP2 are studied. These include correction of vertical detuning with horizontal amplitude by employing multipole correctors in straight sections, changing the betatron phase advances per cell and shifting to another operating point. Because of cross-talk with arc sextupoles, octupole correctors produce a much stronger effect on the detuning than follows from first-order perturbation theory. This can be used to improve the dynamic aperture of the 90°/60° lattice. With this lattice, it is also possible to change to the operating point $Q_x = 90.18$, $Q_y = 76.33$. In the case of 108° horizontal phase advance per cell, the best solution found is a vertical phase advance of 90°.

Geneva, Switzerland
25 October, 1995

*Permanent adress: PPL JINR, Dubna 141980 Russia

Contents:

1 Introduction.

With the standard LPv6 optics both measurement and computation give the maximum stable value of the Courant-Snyder "invariant" $W_x \approx 4.8$ (π)·mm·mrad [1]. The dynamic aperture is therefore marginal at energies above 90 GeV [1,2]. This limitation appears to come from a large value of the vertical tune derivative with the horizontal invariant: $\partial Q_y/\partial W_x = -27.5 \cdot 10^3$, due to which the vertical tune is driven onto an integer value at large horizontal amplitudes. It is worth mentioning that the detuning at large amplitudes is appreciably larger than that predicted from the quoted values of the cross-derivative (supposedly because of contributions from higher order terms—see Fig.1 and discussion thereafter).

In the light of this, two approaches to the problem of improving LEP dynamic aperture can be followed: a) reducing the dependence of vertical tune on horizontal amplitude, either by employing multipole correctors or by changing the arc cell phase advances; b) shifting Q_y farther away from the integer value. These possibilities are studied in Sections 2-5.

Another limitation is associated with Radiative Beta-Synchrotron Coupling (RBSC) [2] (in the standard 90°/60° optics, this effect is most restrictive for vertical motion, but gets stronger for horizontal motion in lattices with higher horizontal phase advance per cell). This effect becomes even more important since the total RF voltage may be lower than planned [3]. Experiments at $W^{\pm}$ energy will probably start with RF configuration similar to the one given in Table 1.1.

Table 1.1

IP	Ncavities·Voltage (MV)	Voltage/IP (MV)
2	32Nb·8.5+ 28Cu·3.03	356.84
4	72NbCu·10.2	734.40
6	32NbCu·10.2+28Cu·3.03	411.24
8	72NbCu·10.2	734.40
Total RF Voltage		2236.88

According to Ref.[4] this voltage provides sufficient RF bucket for beam energy as high as 91 GeV, which was therefore chosen as the reference energy. Though such a choice is not favorable for obtaining large dynamic aperture, reaching the highest possible energy is a priority.

2 Effect of Sextupole Correctors on Detuning with Amplitude.

Presently there are two pairs of sextupole correctors in each of the four high-beta insertions: tilted "bunch train" sextupoles (MSBT) in pits 1 and 5 and upright "pretzel sextupoles" (MSX) in pits 3 and 7. Since the return to pretzel operation is not planned yet, the latter are available for the correction of the cross-derivative. In this section the effect on dynamic aperture of both normal and skew insertion sextupoles will be studied.

2.1 Correction of the Cross-Derivative.

The case of one sextupole pair per superperiod is treated analytically in Appendix 1. Applying these results to the case of normal sextupole correctors one should keep in mind a possible effect of cross-talk with the arc sextupoles. This effect will be discussed later.

Writing the maximum contribution to $\partial Q_y/\partial W_x$ from the correction sextupoles in the form

$$\left.\frac{\partial Q_y}{\partial W_x}\right|_{max} = \beta_x\beta_y(K2L)^2[\, c_x\beta_x + c_y\beta_y \,] \qquad (2.1)$$

one obtains with the standard tune values $Q_x = 90.29$, $Q_y = 76.19$ the coefficients $c_{x,y}$ and the optimum phase advances from the IPs as given in Table 2.1.

Table 2.1

N_{super}	Type	$\phi_x/2\pi$	$\phi_y/2\pi$	c_x	c_y
2	normal	0.036+0.50k	0.149+0.25l	0.171	0.013
4	normal	0.143+0.50k	0.137+0.25l	0.063	0.032
2	tilted	0.161+0.25k	0.024+0.50l	0.020	0.265
4	tilted	0.143+0.25k	0.012+0.50l	0.019	1.065

The number of superperiods N_{super} may be understood here as just the number of sextupole pairs in the whole ring (N_{pair}), k and l are arbitrary (non-negative) integers. As mentioned in Appendix 1, in the case of antisymmetric excitation, the optimal phases, $\phi_x/2\pi$, of normal sextupoles and $\phi_y/2\pi$ of skew sextupoles, are shifted by 0.25.

The data in Table 2.1 show that skew sextupoles are much more efficient than normal sextupoles. This is confirmed by computation with the program ***MAD*** [5]. Table 2.2a shows distances and phase advances from the nearest IP to the existing and additional (marked with asterisk) insertion sextupoles. The β-function values quoted here were taken at the right MSBT and MSX sextupoles in pits 1 and 3 respectively (i.e., they are not the average values).

The residual values of detuning coefficients for the given strength and number of the sextupole pairs in the ring (to be compared with the initial values $\partial Q_x/\partial W_x = 1749$, $\partial Q_y/\partial W_x = -27498$, $\partial Q_y/\partial W_y = 18210$) as well as the corresponding horizontal dynamic aperture of the perfect machine $A_x = (W_x[\mu m])^{1/2}$ in the absence of radiation are presented in Table 2.2b. The contribution of the correction sextupoles to the cross-derivative agrees quite well with the analytic calculations in Appendix 1. This indicates that there is no significant cross-talk between correction and arc sextupoles in the second order.

The phase advances of both existing pretzel sextupole families are far from the optimum for normal sextupoles, the effect of SD.QL4B's being completely negative. The SD.QL9's do reduce the cross-derivative but, since $\beta_x >> \beta_y$, they have a much larger effect on $\partial Q_x/\partial W_x$. Additional sextupoles placed at more favorable phase advances and β-functions near the QL5s seem to be quite efficient (according to ***MAD***'s HARMON and STATIC commands) in correcting the cross-derivative. However the net effect on dynamic aperture is still negative, probably because a horizontal nonlinear resonance is excited (it is difficult to determine the order of the resonance since particles survive only few turns). Though it may be possible to diminish the excitation of this resonance by employing a larger number of correctors, this approach seems hopeless in view of the large contribution of higher order terms to the vertical detuning with horizontal amplitude.

The phase advances of SD.QL9's are almost optimal for the effect of *skew* sextupoles on the cross-derivative but the β-functions are not. As the result the effect of a tilted SD.QL9 on $\partial Q_y/\partial W_x$ is not very significant even for the large value of K2L which was taken. Moreover the net effect on dynamic aperture is highly detrimental. The SBT.QL6 sextupoles (when powered

Table 2.2a

Name	Type	s [m]	$\phi_x/2\pi$	$\phi_y/2\pi$	β_x [m]	β_y [m]
SD.QL4B	normal	75.86	0.424	0.307	22.47	98.02
SD.QL5*	normal	114.0	0.508	0.655	61.89	51.95
SD.QL9	normal	195.4	0.673	1.006	138.0	21.07
SD.QL9	tilted	195.4	0.673	1.006	138.0	21.07
SBT.QL2B	tilted	34.92	0.139	0.177	113.1	21.13
SBT.QL6	tilted	124.0	0.541	0.677	49.12	75.31
SBT.QL6+add*	tilted	124.0	0.541	0.677	49.12	75.31

antisymmetrically) have a more pronounced effect on the cross-derivative but the dynamic aperture is as small as in the previous case. This remains so even if additional SBT.QL6 pairs are installed in pits 3, 7 and the excitation is lowered by half. However it turns out that tilted sextupoles can produce a noticeable effect on detuning at large values of W_x even at a much lower excitation level.

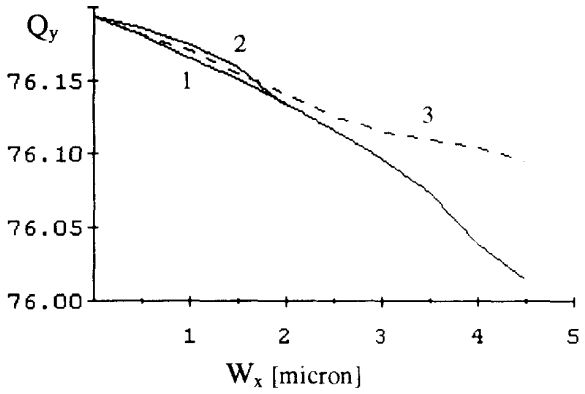

Figure 1. Vertical tune vs. horizontal invariant with: 1 - no insertion correctors; 2 - SD.QL5 normal sextupoles; 3 - SBT.QL6 tilted sextupoles.

2.2 Higher Order Effects.

Fig.1 shows the dependence of the vertical tune Q_y on the horizontal Courant-Snyder invariant W_x found by tracking with ***MAD***, either from phase advance per 10 turns (solid curves) or from FFT plots (dashed curve). Curve 1 was obtained with the LPv6 optics without insertion correctors. At small amplitudes ($W_x \leq 1\mu m$) the slope of the curve corresponds quite well to the calculated cross-derivative value but at large amplitudes it is appreciably larger. The stability limit of $\Delta Q_y/W_x = -4{\cdot}10^4$ m^{-1} might be attributed to higher order effects (but one must be cautious in drawing conclusions since the depth of W_x beating has not been checked). With the normal sextupole SD.QL5 correctors, the detuning (curve 2) initially also follows the corresponding cross-derivative value but at $W_x = 2.2$ μm (the stability limit in this case) it is already larger than in the absence of any additional correctors.

It turns out that, in contrast to normal sextupoles, tilted sextupoles have a favorable effect on detuning at large values of W_x. This is quite noticeable, even at a low excitation. The dashed curve on Fig.1 shows the vertical tune with SBT.QL6's switched on (including additional pairs in pits 3, 7) at K2L = .053 m^{-2}. In this case, the dynamic aperture is almost as large as without correctors. Tracking with the arc sextupoles off shows no visible variation in Q_y (nor particle loss) over a wide range of W_x, indicating that the observed effect is due to cross-correlation between arc and correction sextupoles.

An attempt was made to find a skew sextupole configuration which would reduce detuning without strong resonance excitation, thus improving the dynamic aperture, either by employing a larger number of tilted insertion sextupoles or by introducing a small tilt of the arc sextupoles. No positive result was obtained (in the latter case no correcting effect on detuning was observed). To achieve the desired goal, we need a tool for consistent analysis of the higher order effects.

3 Effect of Octupole Correctors on Detuning with Amplitude.

It is clear that sextupoles are not the best way to correct detuning: the desired effect is second order in their strength whereas the undesirable resonance excitation may occur in the first order and thus

Table 2.2b

N_{pair}	K2L [m^{-2}]	$\partial Q_x/\partial W_x$ [m^{-1}]	$\partial Q_y/\partial W_x$ [m^{-1}]	$\partial Q_y/\partial W_y$ [m^{-1}]	$A_x[\sqrt{\mu m}]$
2	0.608	950	-34195	10515	1.3
2	0.608	-12197	-15808	8765	1.5
2	0.608	-58935	-17769	17281	1.0
2	0.608	-35347	-19440	17548	1.5
2	±0.608	-16015	-25572	17832	-
2	±0.608	-8379	-12914	-3646	1.5
4	±0.304	-10014	-10819	-8048	1.5

dominate the particle dynamics. In this respect, correction of the detuning with octupoles looks more promising.

The contribution of a single octupole to the detuning coefficients is given by the formulas

$$\frac{\partial Q_y}{\partial W_x} = -\frac{\beta_x \beta_y K3L}{16\pi}, \qquad \frac{\partial Q_u}{\partial W_u} = \frac{\beta_u^2 K3L}{32\pi}, \quad u = x, y \tag{2}$$

With the help of ***Mathematica*** [6], we have generated analytical expressions for contribution from an octupole pair per superperiod to the second derivative of vertical tune with the horizontal invariant. These can be found in Appendix 2.

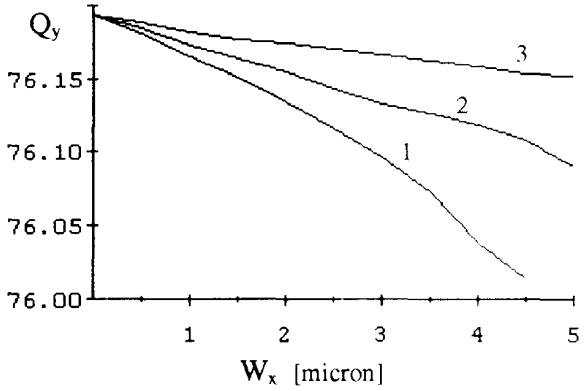

Figure 2. Vertical tune vs. horizontal invariant with OCT.QS2 correctors at K3L = 0; -1.59; -3.26 m^{-3} for the l05p46v6 optics.

3.1 90°/60° lattice.

In LEP there are OCT.QS2 octupole pairs installed around all even IP's, the average value of the product of beta-functions at their location being $\langle\beta_x\beta_y\rangle = 8.47\cdot10^4$ m^2. With the present power supply, their maximum normalized strength at 91 GeV is $|K3L| = 1.6$ m^{-3}, allowing a correction of the cross-derivative by less than $3\cdot10^3$ m^{-1}. However, just as in the case with tilted sextupoles, the effect of octupoles on detuning at large horizontal amplitudes is significantly stronger than might be inferred from the corresponding cross-derivative value. Fig.2 shows the vertical tune with OCT.QS2 strength set in turn to the values K3L = 0, -1.59 and -3.26 m^{-3}. Based on these data, the octupoles contributions to the cross-derivative are estimated to be $1.2\cdot10^4$ m^{-1} and $2.3\cdot10^4$ m^{-1}. These values are a factor 4 larger than follows from the expressions (3) and the ***MAD*** STATIC routine. It turns out that the effect is again mainly due to cross-talk with arc sextupoles. The contribution of higher order terms to $\partial Q_x/\partial W_x$ is less significant. This derivative follows the corresponding first order perturbation theory formula more closely, being equal to $-1.4\cdot10^4$ m^{-1} at K3L = -3.26 m^{-3}.

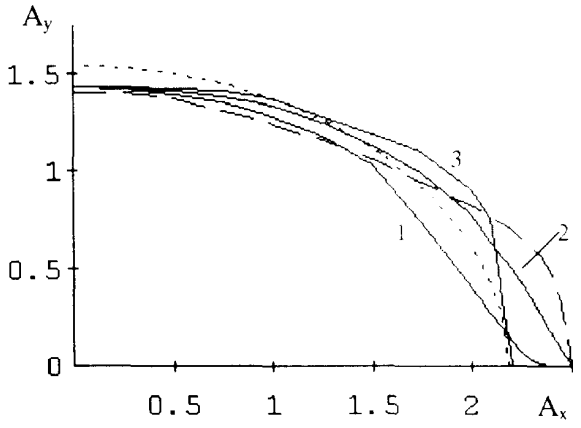

Figure 3. Effect of octupole correctors on the l05p46v6 lattice dynamic aperture at 91 GeV.

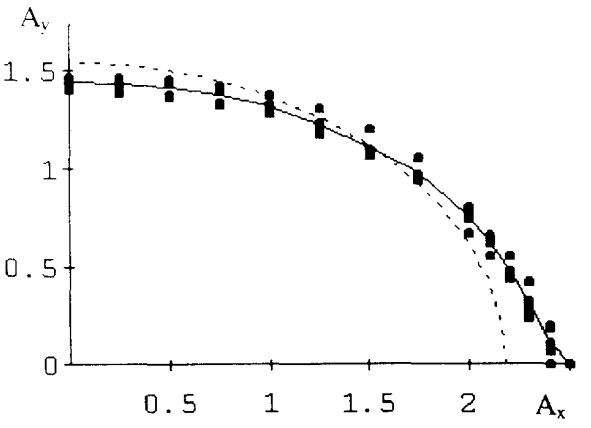

Figure 4. Dynamic aperture at 91 GeV with OCT.QS2 correctors on in presence of misalignments

Fig.3 shows the dynamic aperture the perfect LEP at 91GeV in the A_x-A_y plane, where $A_u = (W_u[\mu m])^{1/2}$, u = x,y. It was computed with the l05p46v6 optics and the RF configuration given in Table 1.1. Curves 1-3 correspond to those in Fig.2. The dotted line is the 10σ ellipse for beam emittances $2\varepsilon_y = \varepsilon_x = 47.5$ nm. As can be seen from the plot, there is little advantage in increasing the OCT.QS2 octupoles strength over the present limit because of excitation of horizontal resonances. It should be noted that although tracking was performed with zero initial energy deviation, the RBSC mechanism excites synchrotron oscillations with amplitude up to $\delta_p = 0.5\%$.

It is possible to improve the dynamic aperture further by installing octupoles in places with large vertical β-function. The dashed line in Fig.3 was obtained with strong (K3L = -10 m^{-3}) octupole correctors placed at ±62m from the even IPs near QS3 quadrupoles, where in the second pit β_x = 50m, β_y = 122m. In this case the vertical tune dependence on horizontal amplitude is practically the same as given by curve 3 in Fig.2. It should be checked that there are no negative side effects from these octupoles when the bunch trains bumps are on.

It may turn out that, in the presence of misalignments, octupoles would excite additional resonances due to errors in phase advances. Fig.4 shows the dynamic aperture calculated with different seeds of quadrupole misalignments with OCT.QS2 correctors on at K3L = -1.59 m^{-3}. The alignment errors were assumed to be $\langle x^2\rangle^{1/2} = \langle y^2\rangle^{1/2} = 0.15$ mm, $\langle psi^2\rangle^{1/2} = 0.24$ mrad. The closed orbit was corrected with accuracy $\langle x_{c.o}^2\rangle^{1/2} = 0.3$ mm, $\langle y_{c.o}^2\rangle^{1/2} = 0.6$ mm at BPM's (this has been made rather worse than in reality just to make the effect of errors more visible), RMS monitor read error being 0.2 mm. The solid curves join average values. Comparison with curve 2 in Fig.3 shows no significant effect of misalignments in the present case. It has also been checked that these octupoles do not reduce the energy acceptance.

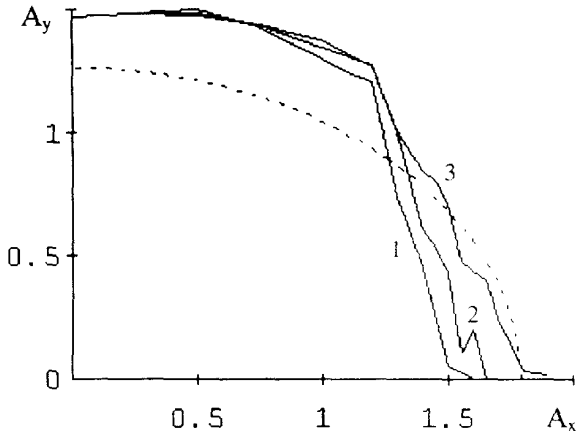

Figure 5. Effect of octupole correctors on the c05r46 (108/60) lattice dynamic aperture at 91 GeV.

3.2 108°/60° lattice.

The dynamic aperture of the 108°/60° lattice is limited at large W_x by the same effect of vertical tune dependence on the horizontal amplitude. The cross-derivative in this case is much larger than for the 90°/60° lattice: $\partial Q_y/\partial W_x = -8.12\cdot10^4$. The dynamic aperture (see curve 1 in Fig.5) is correspondingly smaller, both in absolute value and in relation to σ_x. Fig. 5 shows the effect of OCT.QS2 correctors with strength set equal to he values K3L = 0; -1.59; -10.3 m^{-3} in turn. The last value was found to be the most effective but does not really improve the dynamic aperture. This is still smaller than the 10σ ellipse for beam emittances $2\varepsilon_y = \varepsilon_x = 32$ nm. A more significant improvement can probably be achieved with octupoles installed near the QS3 quadrupoles but these octupoles would have to be even more powerful.

4 Variation of Cell Phase Advances

Figures 5,6 show the dependence of the cross-derivative on arc cell phase advances obtained with the help of ***Mathematica*** (see Appendix 2 in Ref.[7]) under the assumption that the betatron tunes modulo 4 are kept constant (as well as phase advances in the even insertions).. The cross-derivative as a function of μ_x falls off rapidly for μ_x>120°. The μ_x = 135° option has been well

studied (see [7] and references therein) and is of significant interest for LEP2 since it minimises the natural beam emittance. As a function of μ_y the cross-derivative monotonously decreases in absolute value with μ_y increasing and reaches fairly low values at $\mu_y = 90°$.

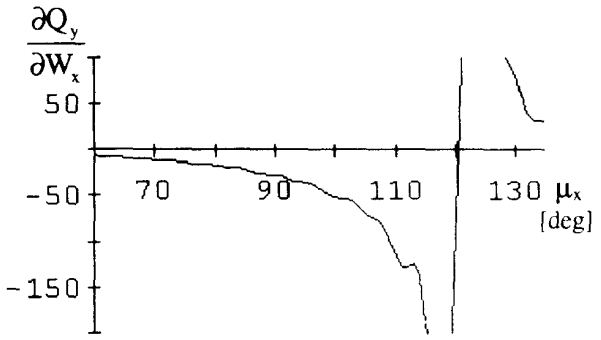

Figure 6. Cross-derivative vs. horizontal phase advance per cell with $\mu_y = 60°$

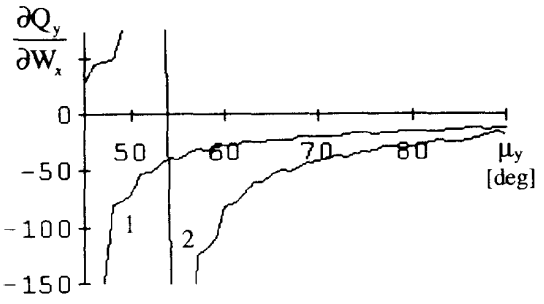

Figure 7. Cross-derivative vs. vertical phase advance with two μ_x values: 1 - 90°, 2 - 108°.

4.1 Comparison of different optics

To study the $\mu_y = 90°$ option in the case of $\mu_x = 90°$ an old s05m46_934 optics was used (with this optics $\beta_x^* = 1.25$m at even IPs, a factor two smaller than in the other optics considered in the present report). For the case of $\mu_x = 108°$ a new optics called y05e46 was matched and compared with l05p46v6 (90°/60°) and C05R46 (108°/60°) optics. Table 4.1 gives values of detuning coefficients and synchrotron integrals responsible for RBSC [2] for these four optics.

Table 4.1

lattice	$\partial Q_x/\partial W_x$	$\partial Q_y/\partial W_x$	$\partial Q_y/\partial W_y$	I_{6x}	I_{6y}
90°/60°	1,750	-27,500	18,210	62.8	207.9
90°/90°	950	-13,930	960	84.5	226.1
108°/60°	23,560	-81,180	75,430	75.4	218.2
108°/90°	23,650	-17,060	11,340	79.2	216.3

Fig. 8 compares the dynamic aperture in A_x - A_y plane, where $A_u = (W_u[\mu m])^{1/2}$, u = x,y, obtained at 91 GeV with the LEP2 RF configuration presented in the Introduction for the four optics under consideration. Dots represent values obtained with different seeds of misalignments. RMS errors and closed orbit correction were as given in subsection 3.1. Dashed lines join average values (with the exception of the 90°/90° case where it corresponds to the perfect machine with $V_{RF} = 2236.9$ MV), solid lines show the dynamic aperture of the perfect machine with total RF voltage $V_{RF} = 2500$ MV. Dotted lines correspond to 10σ beam ellipses.

Comparison of the two optics with $\mu_x = 90°$ shows some gain in dynamic aperture due to higher μ_y only when the RF voltage is sufficiently high. At lower voltage, the dynamic aperture of s05m46_934 lattice is more severely limited by RBSC because of the smaller β_x^* and correspondingly larger I_{6x}. This underlines the necessity of taking RBSC into consideration when choosing β_x^* and β_y^* for high energy operation.

The horizontal dynamic aperture of the 108°/60° lattice is insensitive to both misalignments and RF voltage (as has been already found in Ref.[1]) since it is limited by the systematic integer

resonance $Q_y = 4{\cdot}19$. The dynamic aperture of the 108°/90° lattice seems to be determined by the cooperative effect of imperfection driven resonances and RBSC.

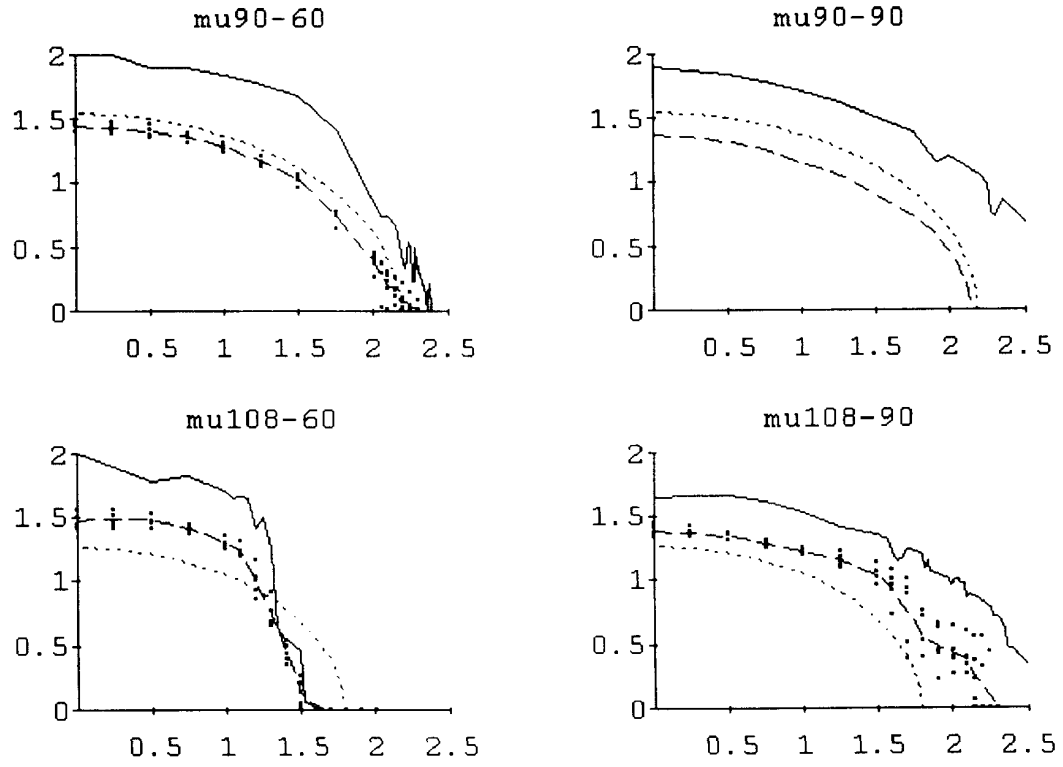

Figure 8. Dynamic aperture in A_x, A_y plane of the four lattices at 91 GeV.

4.2. 108°/90° lattice.

The interest of this lattice is based on the following points:
a) low natural emittance ($\varepsilon_x = 32.6$ nm at 91 GeV) due to $\mu_x = 108°$, necessary for obtaining high luminosity at LEP2 energies;
b) larger horizontal dynamic aperture than with the 108°/60° optics;
c) higher TMCI threshold due to a smaller $<\beta_y>$ in the arcs [8].

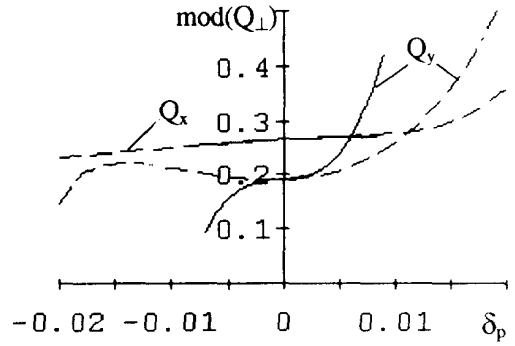

Figure 9. Fractional part of the tunes vs momentum deviation before (solid lines) and after (dashed lines) correction of vertical non linear chromaticity.

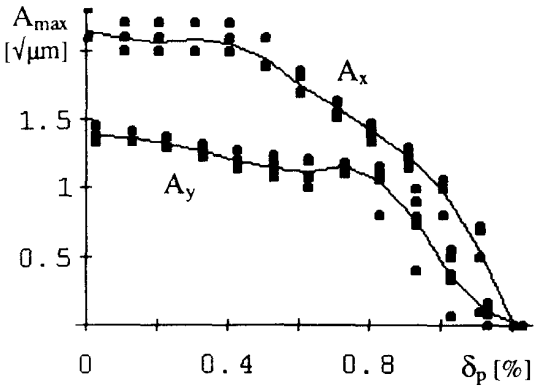

Figure 10. Maximal stable amplitude (square root of the Courant-Snyder invariant in μm) vs. synchrotron amplitude at 91GeV with V_{RF} = 2237MV. Dots representing vertical amplitude at different seeds are slightly shifted to the right.

The proposed YE optics has the same low- and high-beta insertions as the standard LPv6 optics, the nominal tune values being $Q_x = 103.268$, $Q_y = 97.193$. The integer parts of the tunes were chosen odd in order to reduce nonlinear chromaticity [9] since it cannot be corrected with the present connection of SD sextupoles. With equal excitation of all three SD families (and also equal excitation of both SF's) the energy acceptance (in absence of radiation damping) is smaller than 0.8% (see Fig.9). However with a strong radiation damping at 91 GeV it is almost as large as the RF bucket energy width (with exception for one "pathological" seed of misalignment out of the five taken). This may be explained by a stabilizing positive shift of the vertical tune with increasing vertical amplitude (see Table 4.1). But with higher RF voltage the energy acceptance does not become larger, so the value of 1.1% can be considered as maximum achievable without nonlinear chromaticity correction.

If this optics were to be adopted for operation, a proper correction of vertical nonlinear chromaticity with $\mu_y = 90°$ can be achieved by rearranging the SD sextupoles into two families [9]. With normalized gradients in the families KSD1 = -0.333m^{-3}, KSD2 = -0.185 m^{-3}, the energy acceptance may be increased up to 2% and is determined by the RF bucket energy width. It may be argued whether the variation in SD strengths would affect the transverse dynamic aperture. Tracking at 91 GeV shows a slight **increase** in dynamic aperture of the perfect machine due to correction of nonlinear chromaticity. This indicates that the RBSC is a major limiting mechanism in the absence of imperfections.

The YE optics was tested in two machine development (MD) studies on 15/09/95 and 07/10/95. The vertical TMCI threshold with only damping wigglers on and $Q_s = 0.085$ was measured to be 0.505 mA/bunch, so the gain w.r.t. 108°/60° lattice (0.430 mA/bunch under the same conditions [10] but with a **smaller** number of SC RF cavities) turned out to be even larger than ≈13% expected from the ratio of $\Sigma\beta_y Z_y$ for **equal** numbers of RF cavities (see Table 4.2, where data of Ref.[11] were used).

Table 4.2

lattice	$\langle\beta_y\rangle_{arcs}$	$Z_{y,\,arcs}$	$\Sigma_{RF}\,\beta_y Z_y$	$\Sigma_{tot}\,\beta_y Z_y$
108°/60°	86	0.42	30	66
108°/90°	68	0.42	30	59

Another important characteristic of bunch stability is the coherent tune shift with bunch current. It was found to be

$$\frac{dQ_x}{dI_b} = -0.061\ mA^{-1},$$

$$\frac{dQ_y}{dI_b} = -0.130\ mA^{-1},$$

which may be compared with the values -0.066 mA^{-1} and -0.145 mA^{-1} respectively for horizontal and vertical tuneshifts obtained with 90°/60° optics (see Ref.[12]) with $Q_s = 0.102$ and also only damping wigglers on but with 4 **fewer** SC RF units. The 11.5% reduction in vertical tuneshift with current is again somewhat larger than might have been expected: the reduction in $\Sigma\beta_y Z_y$ should be partially compensated due to 6% bunch shortening (decrease in momentum compaction factor α_M from $1.9\cdot10^{-4}$ to $1.4\cdot10^{-4}$ should overcome smaller Q_s). Even more suprising is the 9% reduction in horizontal tuneshift with current since the expected drop in $\Sigma\beta_x Z_x$ due to larger μ_x is only 0.6%. A possible explanation of the observed changes is a stronger bunch lengthening due to smaller α_M (and/or larger **longitudinal** impedance with new SC RF cavities in). Unfortunately the streak camera was out of operation during these machine development periods and the bunch length was not measured.

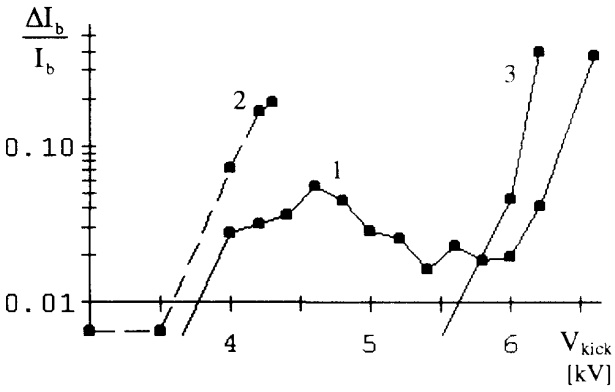

Figure 11. Relative bunch current loss vs. IK3E kicker voltage: 1 - $\beta_y^* = 0.09$m, no wigglers; 2 - $\beta_y^* = 0.09$m, emittance and damping wigglers on; 3 - $\beta_y^* = 0.05$m, no wigglers.

In the second MD, the dynamic aperture of the squeezed optics at 45.6 GeV was measured using the injection kicker IK3E. The kicker calibration at this energy is 0.032 mrad/kV, at its location $\beta_x = 126$ m, $\alpha_x = 2.7$. The observed loss in bunch current is plotted in Fig.11 as a function of the kicker voltage. The solid curves join values obtained with wigglers off ($\varepsilon_x = 8.3$nm, $\sigma_E = 0.72\cdot10^{-3}$), the dashed one—with the emittance and damping wigglers on ($\varepsilon_x = 23.6$nm, $\sigma_E = 1.42\cdot10^{-3}$).

With wigglers switched off the losses reached some 40% at $V_{kick} = 6.6$kV with $\beta_y^* = 0.09$m and at $V_{kick} = 6.2$kV with $\beta_y^* = 0.05$m, which gives for the horizontal dynamic aperture $A_x = 2.37\ \sqrt{\mu}$m and $A_x = 2.23\ \sqrt{\mu}$m respectively in reasonable agreement with the predictions.

Some measurements with wigglers on were made only for $\beta_y^* = 0.09$m and showed significant (about 20%) losses already at $V_{kick} = 4.2$ kV. Without wigglers some losses at this voltage were seen also, but having reached a maximum of about 5% at $V_{kick} = 4.6$ kV they went down. The reduction was well above the random and roundoff errors of ~1% in measuring $\Delta I_b / I_b$ in that region.

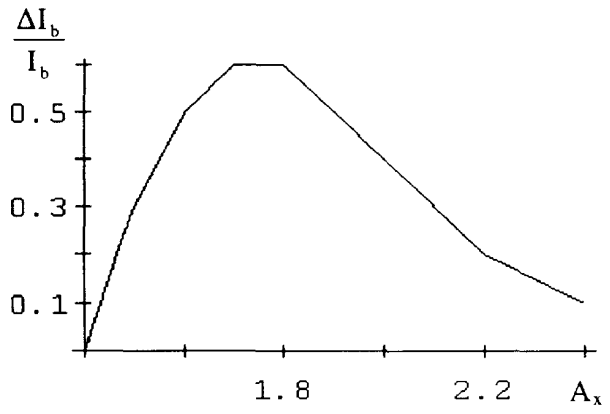

Figure 12. Expectation value of relative number of particles trapped into resonant islands vs. normalized amplitude of oscillation excited by the kick

These observations may be explained by invoking the presence of third integer resonance islands at the radius in phase space corresponding to the acquired betatron amplitude (the Courant-Snyder invariant which corresponds to $V_{kick} = 4.6$ kV is $W_x = 2.73$ μm; the horizontal tune being $Q_x = Q_{x0} + \partial Q_x/\partial W_x \cdot W_x = 103.264 + 2.1 \cdot 10^4 \cdot 2.73 \cdot 10^{-6} = 103.32$).

With misalignments and the closed orbit correction as cited in section 3.1 the typical width of the islands is $\Delta A_x = 0.5$; so particles can survive in them for quite a long time even with wigglers on (for more than 1000 turns, as tracking with quantum fluctuations shows). The rough estimate of probability of trapping particles into the islands in presence of strong radiation damping (corresponding to beam energy 91GeV) but without quantum excitation is shown in Fig. 12. At maximum it is as high as 60%. Therefore the following scenario of particle losses seems possible: when the kicker voltage is high enough to throw particles into a resonant island, particles trapped there can get out of the (dynamic) aperture due to quantum fluctuations or another mechanism. With increasing kicker voltage the number of trapped particles gets smaller which reduces the losses.

When the wigglers are switched on the losses can be intensified due to stronger quantum fluctuations, especially due to increased energy spread

At $\beta_y^* = 0.05$m no losses at the intermediate kicker voltages were observed (with wigglers off), which can be explained by more thorough closed orbit and chromaticity correction and/or displacement of islands in the phase space.

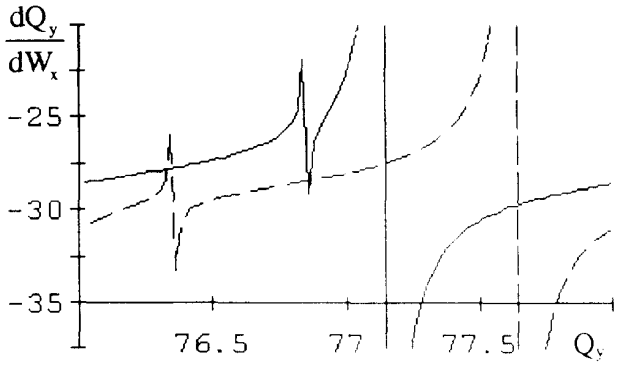

Figure 13. Cross-derivative (in mm^{-1}) vs vertical tune with horizontal tune: $Q_x = 90.3$ (solid curve) and $Q_x = 91.3$ (dashed curve).

5 Shifting Q_y up

Another conceivable solution of the problem with the 90°/60° lattice dynamic aperture is to choose different tune values. As can be seen from Fig.13 (obtained under the same assumptions as Figs. 6,7) there is little possibility to reduce detuning unless moving close to the systematic $Q_x - 2Q_y = 64$ resonance. Hence one should choose the operating point so as to provide a larger room for the tune shift.

The simplest solution is to pull the vertical tune a little farther from the integer value. According to simulations [13] the point $Q_x = 90.18$, $Q_y = 76.33$ is as good for the coherent beam-beam effect as the standard one (this was confirmed in a test physics run with $Q_x = 90.18$, $Q_y = 76.3$ [14]). In Fig.14 the dynamic aperture of the standard optics with shifted tunes is shown in the A_x-A_y plane. It practically coincides with the 10σ beam ellipse (dotted curve) for both the perfect machine (solid curve) and misaligned ones (dashed curve joins mean values).

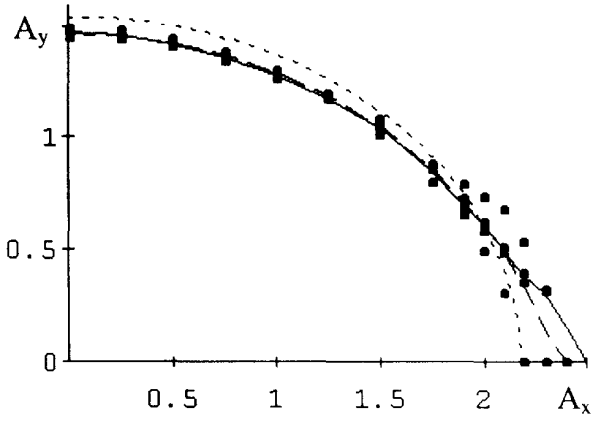

Figure 14. Dynamic aperture of the l05p46v6 optics at 91 GeV with $V_{RF} = 2.237$ GV and betatron tunes shifted to operation point $Q_x = 90.18$, $Q_y = 76.33$

It was not checked but seems quite probable that transition to such fractional tunes would be beneficial in the cases of 108°/60° and 108°/90° optics as well.

6 Summary

- The dynamic aperture of the 90°/60° optics at LEP2 energies is limited by vertical detuning with horizontal amplitude and Radiative Beta-Synchrotron Coupling (beating of the vertical amplitude when the tune approaches the integer value enhances the RBSC). It is marginal for operation at the upper energy limit determined for a given RF voltage by the quantum lifetime.
- The 90°/60° dynamic aperture can be made practically adequate either by changing to the operating point $Q_x = 90.18$, $Q_y = 76.33$ or by employing octupole correctors. Because of cross-talk with the arc sextupoles, the effect of the octupoles on detuning at large horizontal amplitudes was found to be much stronger than expected from first order perturbation theory.
- In the case of 108°/60° optics, the horizontal dynamic aperture is not sufficient for high energy operation. It is insensitive to RBSC (so cannot be improved by raising RF voltage) and is limited mainly by very strong vertical detuning with horizontal amplitude.
- The 108°/90° optics is a promising option for LEP2 because of its significantly larger horizontal dynamic aperture (up to 12σ) and higher TMCI threshold. Both of these predictiions have been borne out in experiments on LEP.

7 Acknowledgements

The author is grateful to J. Gareyte J.M. Jowett, F. Ruggiero, A. Verdier for permanent interest and clarifying discussions. P. Collier, J.M. Jowett and others participated in the experiments on the 108°/90° optics. (Some final editing of this report was done by J.M. Jowett.)

References

1. F.Ruggiero, "Dynamic Aperture for LEP 2", *in* Proc. 5th Workshop on LEP Performance, Chamonix, 1995, p.164.
2. J.M. Jowett, "Dynamic Aperture for LEP: Physics and Calculations", *in* Proc. 4th Workshop on LEP Performance, Chamonix, 1994, p.47.
3. G.Geschonke, private communication.
4. J.M. Jowett, "RF Voltages and Beam Energy for Three LEP2 Optics", CERN LEP2 Note 95-30 (1995)

5. H.Grote, F.C.Iselin, "The MAD Program. Version 8.10. User's Reference Manual", CERN/SL/90-13 (AP) (Rev. 3) 1993.
6. S.Wolfram, "Mathematica. A System for Doing Mathematics by Computer", 2nd ed., Addison-Wesley, 1991.
7. Y.Alexahin, "A Study of the Low Emittance Lattice for LEP2", CERN SL/94-46 AP (1994)
8. A.Verdier, "Optics Considerations for LEP2" *in* Proc. 5th Workshop on LEP Performance, Chamonix, 1995, p.160.
9. A.Verdier, "Chromaticity", *in* Proc. CAS 4th Advanced Accelerator Physics Course, Noordwijkerhout, Netherlands, 1991, Ed.S.Turner, CERN 92-01, p.204 (1992).
10. M.Meddahi, private communication.
11. D.Brandt et al. "Measurement of Impedance Distributions and Instability Thresholds in LEP". CERN-SL-95-34 AP (1995).
12. B.Zotter, "The LEP Impedance Model", SL-Note-95-81 AP (1995).
13. E.Keil, "Simulations for Q_x>70 and Q_y>76", *in* Proc. 1st Workshop on LEP Performance, Chamonix, 1991, p.147.
14. H.Schmickler, private communication.

Appendix 1. Cross-Derivative Due to a Sextupole Pair.

In the case of one pair of symmetrically excited normal sextupoles in each of the N_{super} superperiods the cross-derivative is given by the formula

$$\frac{\partial Q_y}{\partial W_x} = N_{super}\frac{\beta_x\beta_y(K2L)^2}{32\pi}[2\beta_x\frac{\cos(\pi q_x)+\cos(2\phi_x-\pi q_x)}{\sin(\pi q_x)}+$$
$$\beta_y\frac{\cos(\pi q_x-2\pi q_y)+\cos(2\phi_x-4\phi_y-\pi q_x+2\pi q_y)}{\sin(\pi q_x-2\pi q_y)}- \qquad (A1.1)$$
$$\beta_y\frac{\cos(\pi q_x+2\pi q_y)+\cos(2\phi_x+4\phi_y-\pi q_x-2\pi q_y)}{\sin(\pi q_x+2\pi q_y)}]$$

where $2\phi_x$, $2\phi_y$ are the betatron phase advances between sextupoles in a pair, $q_x = Q_x/N_{super}$, $q_y = Q_y/N_{super}$ are betatron tunes per superperiod, K2L is the normalized integrated strength of a sextupole and W_x is the Courant-Snyder invariant (twice the action variable).

For the purpose of correcting negative cross-derivative the phase advances should be chosen so as to maximise the contribution from correction sextupoles. The $\partial Q_y/\partial W_x$ from Eqn.(A1.1) being a single harmonic function in both ϕ_x and ϕ_y, all its extrema are given by the equations

$$\sin(2\phi_x-\pi q_x)=\sin(4\phi_y-2\pi q_y)=0 \qquad (A1.2)$$

The maximum value is:

$$\left.\frac{\partial Q_y}{\partial W_x}\right|_{max} = N_{super}\frac{\beta_x\beta_y(K2L)^2}{32\pi}[\,2\beta_x(\,|\csc(\pi q_x)|+\cot(\pi q_x)\,)+$$
$$\beta_y|\csc(\pi q_x-2\pi q_y)-\csc(\pi q_x+2\pi q_y)|+\beta_y(\cot(\pi q_x-2\pi q_y)-\cot(\pi q_x+2\pi q_y))] \qquad (A1.3)$$

With antisymmetrical excitation the maximal value is the same and is reached at ϕ_x shifted by $\pi/2$ and unchanged ϕ_y.

In the case of skew sextupoles the above formulas can be used with interchanged indices.

Appendix 2. Hori-Deprit Algorithm for 2DoF Nonlinear Motion

This appendix has the format of a Mathematica notebook. Hereafter the plain text is printed in a roman font, input and output are shown in bold and regular typewriter fonts:

```
Off[General::spell]; Off[General::spell1];
```

■ Introduction

This notebook is intended to be a tool for easily finding the 2DoF Hamiltonian normal form and the corresponding phase space transformation by making use of the Hori-Deprit algorithm as presented by Leo Michelotti in his brilliant lecture "Introduction to the Nonlinear Mechanics Arising from Magnetic Multipoles", FERMILAB-Conf-86/30, March 1986. The present version is limited to the nonresonant case.

■ How to use this notebook

To reduce the computation time (or make it at all possible) it is important to proceed in a certain order. The initialization cells contain the most general relations necessary for performing normalization procedure.

The original Hamiltonian should be specified by the user according to the problem considered. At the beginning it is better not to give too much detail of the structure of coefficients

of basis functions (see hereafter a simple example of a normal octupole nonlinearity). Having specified the original Hamiltonian

H = Sum[eps^n*h[n]/n!, {n,nh}]

(it is not necessary to introduce the small parameter **eps** explicitly, it may be set to 1), one can normalize it up to the order **nmax** (not related to **nh**) by evaluating **k[0,nmax]** or any expression containing this coefficient. Lower order coefficients are evaluated and stored in the process. The normalized Hamiltonian is then found as

K = Sum[eps^n*k[0,n]/n!, {n,nmax}],

It is advisible at this point to extract from **K** (or **rhs[n]**) the interesting terms for further manipulations.

If the phase space trajectories are of interest one can map from the new dynamic variables into the original ones (in the nonresonant case) in the following way

zold = znew+Sum[eps^n*zo[0,n]/n!, {n,nmax}].

Having found the desired expressions in a general form, one can use them for subsequent analysis, for example in the thin lens approximation.

■ **Basis functions of dynamical variables**

With action-angle variables (**J[i], d[i]**), **i = 1,nd** (**nd = 2** presently) as the coordinates in the phase space the basis functions may be chosen in the form:

f[e_List, m_List]:= Product[J[i]^(e[[i]]/2), {i,1,nd}]*Cexp[I*Sum[d[i]*m[[i]], {i,1,nd}]];

We will not use this explicit definition until necessary. It is sufficient to define the Poisson brackets with them but first the Poisson brackets themselves should be introduced:

```
pb[a_,b_]:=-pb[b,a]; pb[a_+b_,c_]:=pb[a,c]+pb[b,c];
pb[a_,a_]:=0; pb[a_,b_]:=0 /; FreeQ[a,f[e_,m_]];
pb[a_*b_,c_]:=a*pb[b,c] /; FreeQ[a,f[e_,m_]];
pb[ f[el_List,ml_List], f[e2_List,m2_List]]:=
I/2*(e2[[1]]*ml[[1]]-el[[1]]*m2[[1]])*f[el+e2-{2,0},ml+m2]+
I/2*(e2[[2]]*ml[[2]]-el[[2]]*m2[[2]])*f[el+e2-{0,2},ml+m2];
```

To deal with products of the basis functions *Mathematica*'s notion of upvalues can be employed:

```
f[el_,ml_]*f[e2_,m2_] ^:= f[el+e2,ml+m2];
f[e_,m_]^n_ ^:= f[n*e, n*m];
```

Now we can define action of the trajectory integration operator **tInt=1/D** on the functions containing basis vectors. This operator is the inverse to directional (Lie) derivative operator **D=d/d(theta)+q[i]*d/d(d[i])**, where **q[i]** are unperturbed tunes, **theta=2Pi*s/Circumference** is generalized azimuth

```
tInt[b_+c_]:=tInt[b]+tInt[c];
tInt[f[e_,m_]*a_]:=f[e,m]*ti[m,a] ;
ti[m_,a_*b_]:=a*ti[m,b] /; NumberQ[a];
tInt[0]:=0;
```

where the operator **ti[m,a]=Integrate[a*g[m, t-t'], {t', 0, 2Pi}]** was introduced with Green function

g[m,t]=Cexp[I*m.q*(Pi*Sign[t]-t)]/(2I*Sin[Pi*m.q]);

g[0,t]=(Pi*Sign[t]-t)/2Pi.

Also, we should construct an operator which projects out terms with a particular dependence on angle variables and an averaging operator:

```
pro[m_,b_+c_]:=pro[m,b]+pro[m,c];
pro[m_,a_*f[e_,n_]]:=a*f[e,n]*If[n==m,1,0];
aver[a_+b_]:=aver[a]+aver[b];
aver[a_*b_]:=a*aver[b] /; NumberQ[a];
```

```
aver[ f[e_,m_]*b_]:=f[e,m]*aver[b] ;
ti[m_, aver[a_]*b_]:=aver[a]*ti[m,b];
aver[a_]:=a /; NumberQ[a];
aver[a_*aver[b_]]:=aver[a]*aver[b];
pro[m_,0]:=0
```

From the particular form of the Greenfunction follow simplifying relations

```
aver[ ti[m_, a_]]:=aver[a]/(I m.q) /;m=!=0;
aver[ ti[{0,0}, a_]]:=0;
```

■ Deprit's equations

Let **h[n]** be the **n**-th derivative of the perturbation part in the initial Hamiltonian **H** with respect to some small parameter, **k[0,n]** be that of the new (normalized) Hamiltonian **K** and **S** be the Lie generator of transformation from the new canonical variables back to the original ones. These functions are interrelated by Deprit's equations:

```
k[m_Integer,n_Integer]:=Sum[Binomial[m-1,j-1]*
pb[s[j],k[m-j,n]],{j,1,m}] /; m>0;
sk[n_Integer]:=Sum[Binomial[n-1,j-1]*k[j,n-j], {j,1,n-1}];
sh[n_Integer]:=Sum[Binomial[n-1,j-1]*pb[h[n-j],s[j]],
{j,1,n-1}];
rhs[n_Integer]:=rhs[n]=h[n]+sh[n]-sk[n];
k[0,n_Integer]:=k[0,n]=aver[ pro[{0,0},Expand[rhs[n]]]];
s[n_Integer]:=s[n]=tInt[ Expand[rhs[n] -k[0,n] ]];
```

■ The phase space transformation

The phase space vector **z={d[1], J[1], d[2], J[2]}** can be introduced via its adjoint operator action on the basis functions (**adz[f]=pb[z,f]**):

```
adz[b_+c_]:=adz[b]+adz[c];
adz[a_*f[e_List, m_List]]:=
a*{e[[1]]/2*f[e-{2,0},m], -I*m[[1]]*f[e,m],
   e[[2]]/2*f[e-{0,2},m], -I*m[[2]]*f[e,m]} ;
adz[0]:={0,0,0,0};
```

Derivatives of the phase space vector in the old coordinates with respect to the small parameter, **zo[0,n]**, may then be found from the following relations (first we take care to extend the Poisson bracketing on lists):

```
Attributes[pb]={Listable};
zo[0,1]:=adz[s[1]];
zo[0,n_Integer]:=zo[0,n]=adz[s[n]]-
Sum[Binomial[n-1,m]*zo[m,n-m], {m,1,n-1}];
zo[m_Integer,n_Integer]:=
Sum[Binomial[m-1,j-1]*pb[s[j],zo[m-j,n]],{j,1,m}]/;m=!=0;
```

■ Perturbing Hamiltonian

If no particular nonlinear term dominates, it is convenient (but by no means necessary) to order the perturbative part of the Hamiltonian as follows

h[n]=Sum[cf[m,n+2-m]*x1^m*x2*(n+2-m), {m,0, n+2}]

so that **n=1** corresponds to sextupolar field, **n=2** - to octupolar, and so on. For the sake of brevity the factor **R/Bro** was included in the coefficients **cf[m1,m2].**

We may express now **x1, x2** through the basis functions of action-angle variables according to the relation

x1=-I*Sqrt[beta[1]/2]*(Exp[I*psi[1]]*f[{1,0},{1,0}]-Exp[-I*psi[1]]*f[{1,0},{-1,0}]]

and the analogeous one for **x2**, where **psi[i]=phi[i]-q[i]*theta, phi[i]** and **q[i]** are the betatron phase advances and tunes.

```
h[n_Integer]:=Expand[ Sum[ cb[{m,n+2-m}]*
(Exp[I*psi[1]]*f[{1,0},{1,0}]-
Exp[-I*psi[1]]*f[{1,0},{-1,0}])^m*
(Exp[I*psi[2]]*f[{0,1},{0,1}]-
Exp[-I*psi[2]]*f[{0,1},{0,-1}])^(n+2-m),
{m, 0, n+2}]];
```

where **cb[m]=cf[m]* Product[(-I*Sqrt[beta[i]/2])^m[[i]],{i,1,2}]**

■ Resonance coefficients

The above iterative procedure may be continued up to the order nr in which a "sufficiently close" resonance is encountered. To proceed further, the corresponding term in **rhs[nr]** should be relegated to **k[0,nr],** which requires a more sophisticated algorithm. All we can do with the present one is to fish out terms which drive resonance **nx*qx+ny*qy=p** with the help of projection operator (Fourier transform and adding complex conjugate kept in mind)

```
kres=pro[{nx,ny}, Expand[ rhs[nr]]]/nr!;
```

■ Second Order Effects Due to Octupolar Field

Let us consider for example the case of a normal octupole field:

```
cb[{m_,n_}]:=0 /; m+n=!=4 (* only octupoles present *)
cb[{3,1}]=0; cb[{1,3}]=0; (* no skew-octupoles *)
```

Let us first have a look at the detuning (first order in octupole strength) terms in the new Hamiltonian

```
dq1dw1=Coefficient[ k[0,2], f[{4,0},{0,0}]]/2;
dq2dw1=Coefficient[ k[0,2], f[{2,2},{0,0}]]/4;
dq2dw2=Coefficient[ k[0,2], f[{0,4},{0,0}]]/2;
```

Now compute the second derivatives of the vertical tune with horizontal and vertical Courant-Snyder invariants, 6th order difference resonance driving term and nonlinear part of the map:

```
ddq2dw1dw1=Coefficient[ k[0,4], f[{4,2},{0,0}]]/48;
ddq2dw1dw2=Coefficient[ k[0,4], f[{2,4},{0,0}]]/48;
ddq2dw2dw2=Coefficient[ k[0,4], f[{0,6},{0,0}]]/8;
kres2m4=pro[{2,-4}, Expand[rhs[4]]]/24;
disz=Sum[zo[0,n]/n!,{n,4}];
```

Now it is a good time to express **cb**'s through the multipole coefficients (following Michelotti we use the "Fermilab convention" for them) and beta-functions:

```
cf[{m_Integer,n_Integer}]:= Binomial[m+n,n]/(m+n)*
   If[Mod[n,2]==0, (-1)^(n/2)*b[m+n-1],
     (-1)^((n+1)/2)*a[m+n-1]]*(n+m-2)!;
cb[m_List]:=cf[m] Product[ (-I Sqrt[beta[i]/2])^m[[i]], [i,1,2]];
```

■ Thin octupoles

In the thin lens approximation, the multipole arrangement can be represented by a list of integrated strengths. All functions entering integrands should be given as lists of values at the multipole locations.

Let us return to the original Hamiltonian expansion in terms of basis functions. Coefficients at **f[e_,m_]** contain exponentials **Exp[-I m.q*theta]** which may be omitted since they follow transmutations of the **m** index of the adjoint basis function and can be easily restored if necessary.

In the 'shear' (alias 'detuning') terms in the Hamiltonian they completely cancel out. In the resonance driving term one should then take a simple average instead of Fourier transform.

With this convention the integral operators for **ns** thin multipoles are reduced to the following sums:

```
tKern[m_List]:=(Cos[Pi*m.q]*IdentityMatrix[ns]+
Exp[ I*Pi*m.q]*Table[If[i>j,1,0],{i,ns},{j,ns}]+
Exp[-I*Pi*m.q]*Table[If[i<j,1,0],{i,ns},{j,ns}])/
(2I*Sin[Pi*m.q]);
tKern[[0,0]]:=Table[Sign[i-j]*Pi-th[[i]]+th[[j]],
[i,ns],{j,ns}]/(2Pi);
ti[m_List,a_List]:=Expand[ tKern[m].a];
aver[a_List]:=Apply[Plus,a]/(2Pi);
```

Consider one pair (per superperiod) of symmetrically excited octupoles (the convention on phase shifts is in effect!)

```
ns=2;
q={qx,qy};
beta[1]={btx,btx};
beta[2]={bty,bty};
b[3]={k3L,k3L}/6;
psi[1]={phx,2Pi*qx-phx};
psi[2]={phy,2Pi*qy-phy};
```

First let us check detunings:

```
dq1dw1
   2
btx  k3L
--------
 16 Pi
dq2dw1
-(btx bty k3L)
--------------
     8 Pi
ddq=Simplify[ Expand[ ComplexExpand[ddq2dw1dw1]]]
   3        2                    2    2    2
btx  bty k3L  Cot[2 Pi qx]   btx  bty  k3L  Cot[2 Pi (qx - qy)]
--------------------------- + ---------------------------------- -
          64 Pi                                256 Pi

    2    2    2
 btx  bty  k3L  Cot[2 Pi qy]
 ---------------------------- -
            64 Pi

    2    2    2
 btx  bty  k3L  Cot[2 Pi (qx + qy)]
 ---------------------------------- +
              256 Pi

    3        2
 btx  bty k3L  Cos[4 phx - 2 Pi qx] Csc[2 Pi qx]
 ---------------------------------------------- +
                      64 Pi
```

```
    2    2    2
(btx  bty  k3L  Cos[2 (2 phx - 2 phy - Pi qx + Pi qy)]

   Csc[2 Pi (qx - qy)]) / (256 Pi) -

   2    2    2
btx  bty  k3L  Cos[4 phy - 2 Pi qy] Csc[2 Pi qy]
------------------------------------------------ -
                  64 Pi

    2    2    2
(btx  bty  k3L  Cos[4 phx + 4 phy - 2 Pi qx - 2 Pi qy]

   Csc[2 Pi (qx + qy)]) / (256 Pi)
```